

Supporting Information

Biotinylated Polymer-Ruthenium Conjugates: In Vitro and In Vivo Studies in a Triple-Negative Breast Cancer Model

Leonor Côrte-Real ¹, Ana Rita Brás ^{1,2,3}, Adhan Pilon ¹, Nuno Mendes ⁴, Ana Sofia Ribeiro ⁴, Tiago D. Martins ⁵, José Paulo S. Farinha ⁵, M. Conceição Oliveira ⁵, Fátima Gärtner ⁴, M. Helena Garcia ¹, Ana Preto ^{2,3} and Andreia Valente ^{1,*}

¹ Centro de Química Estrutural, Institute of Molecular Sciences and Departamento de Química e Bioquímica, Faculdade de Ciências, Universidade de Lisboa, Campo Grande, 1749-016 Lisboa, Portugal; ldcortereal@fc.ul.pt (L.C.-R.); pg31015@alunos.uminho.pt (A.R.B.); adpilon@fc.ul.pt (A.P.); mhgarcia@fc.ul.pt (M.H.G.)

² Centre of Molecular and Environmental Biology, Department of Biology, University of Minho, Campus de Gualtar, 4710-057 Braga, Portugal; apreto@bio.uminho.pt

³ Institute of Science and Innovation for Bio-Sustainability, University of Minho, Campus de Gualtar, Edifício 18, 4710-057 Braga, Portugal

⁴ i3S—Instituto de Investigação e Inovação em Saúde, Universidade do Porto, 4200-135 Porto, Portugal; nmendes@ipatimup.pt (N.M.); aribeiro@ipatimup.pt (A.S.R.); fgartner@ipatimup.pt (F.G.)

⁵ Centro de Química Estrutural, Institute of Molecular Sciences and Department of Chemical Engineering, Instituto Superior Técnico, Universidade de Lisboa, Av. Rovisco Pais, 1049-001 Lisboa, Portugal; tiagodmartins@tecnico.ulisboa.pt (T.D.M.); farinha@tecnico.ulisboa.pt (J.P.S.F.); conceicao.oliveira@tecnico.ulisboa.pt (M.C.O.)

* Correspondence: amvalente@fc.ul.pt

FT-IR spectra

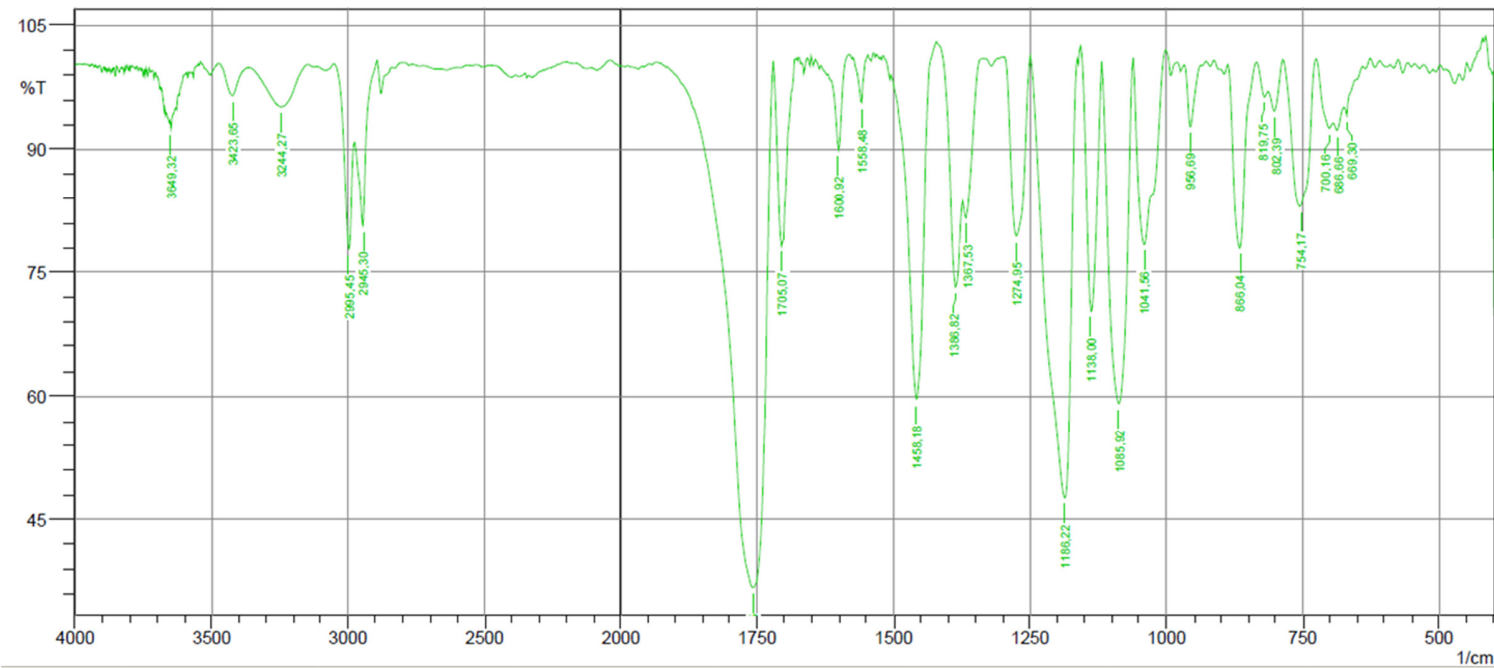


Figure S1. FT-IR spectrum of Ligand L1.

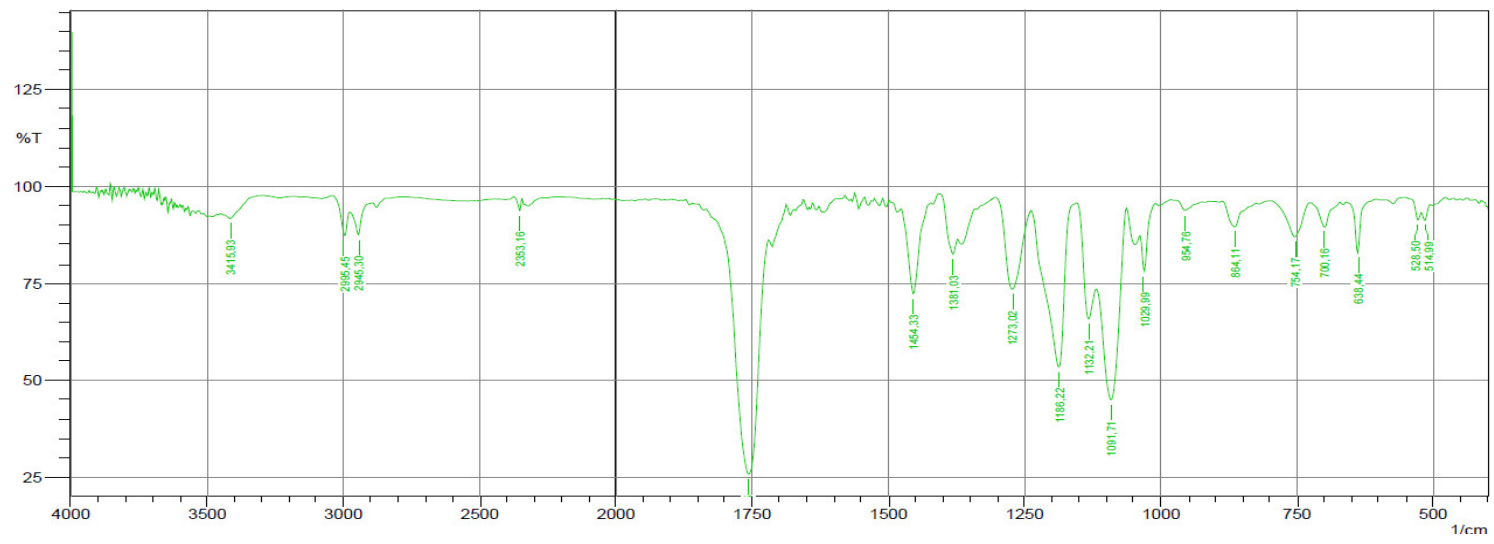


Figure S2. FT-IR spectrum of Complex 1.

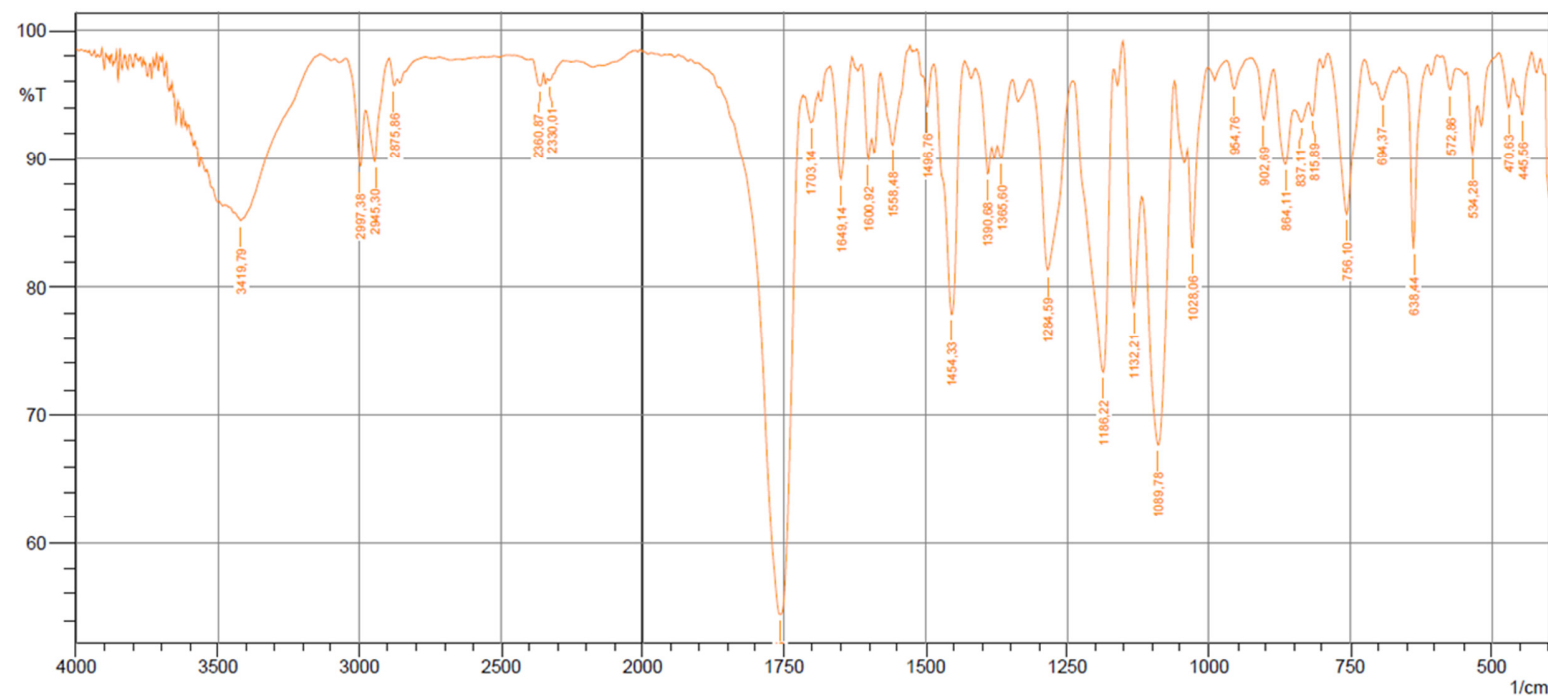


Figure S3. FT-IR spectrum of complex **2**.

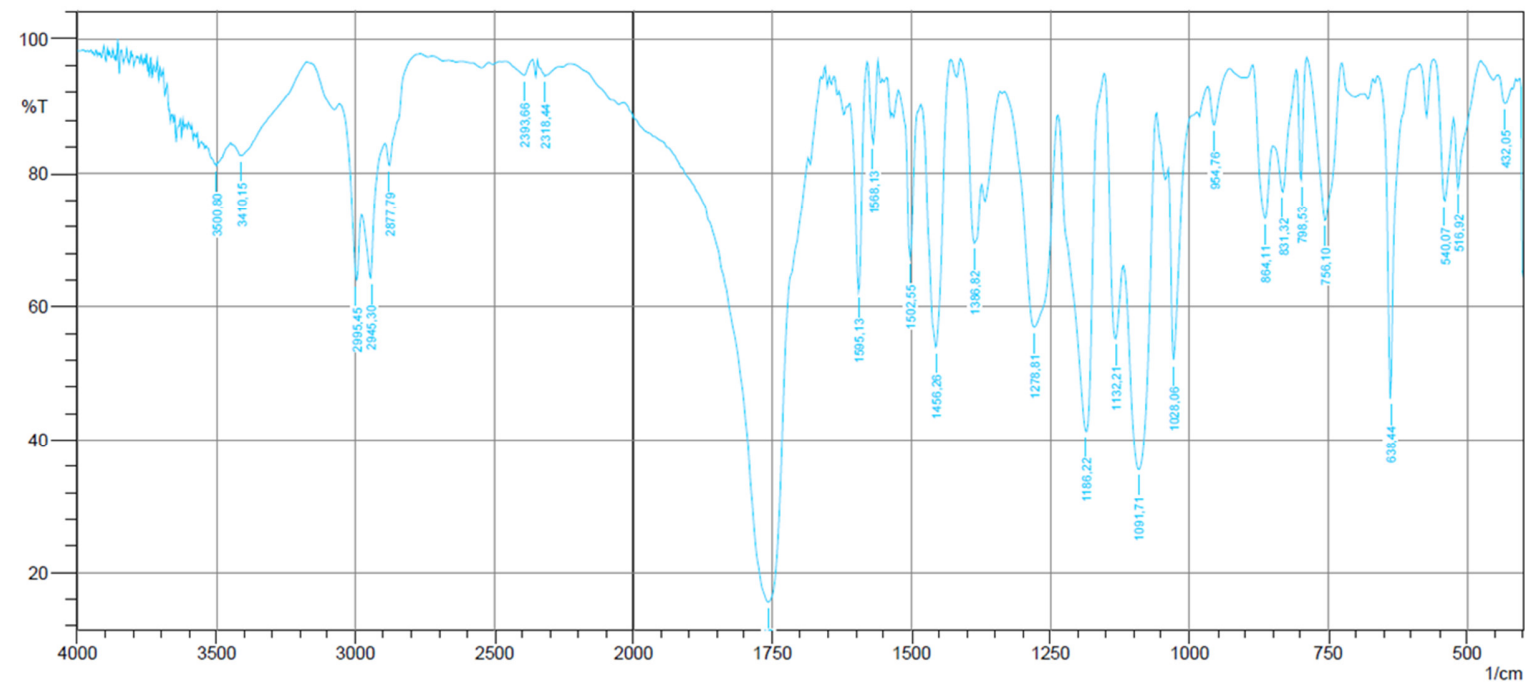


Figure S4. FT-IR spectrum of complex 3.

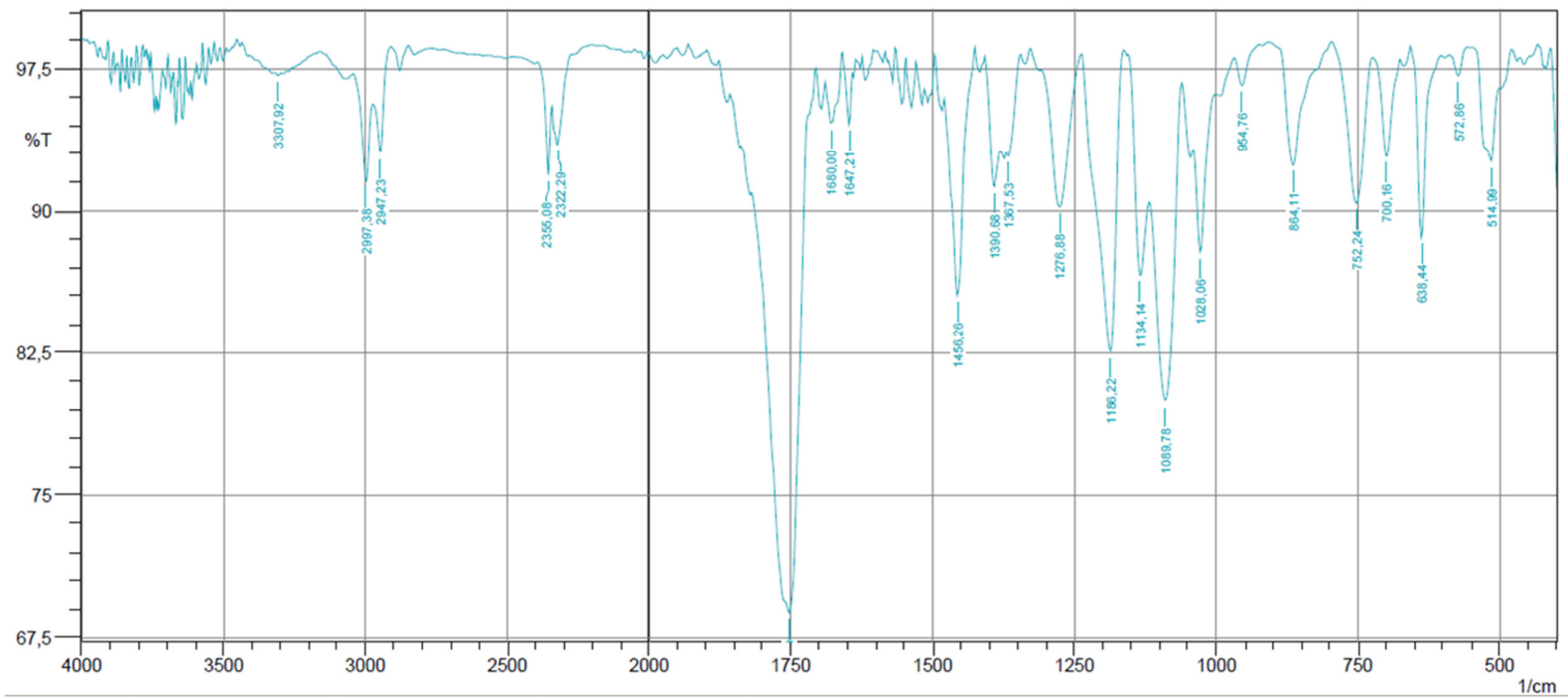


Figure S5. FT-IR spectrum of complex 4.

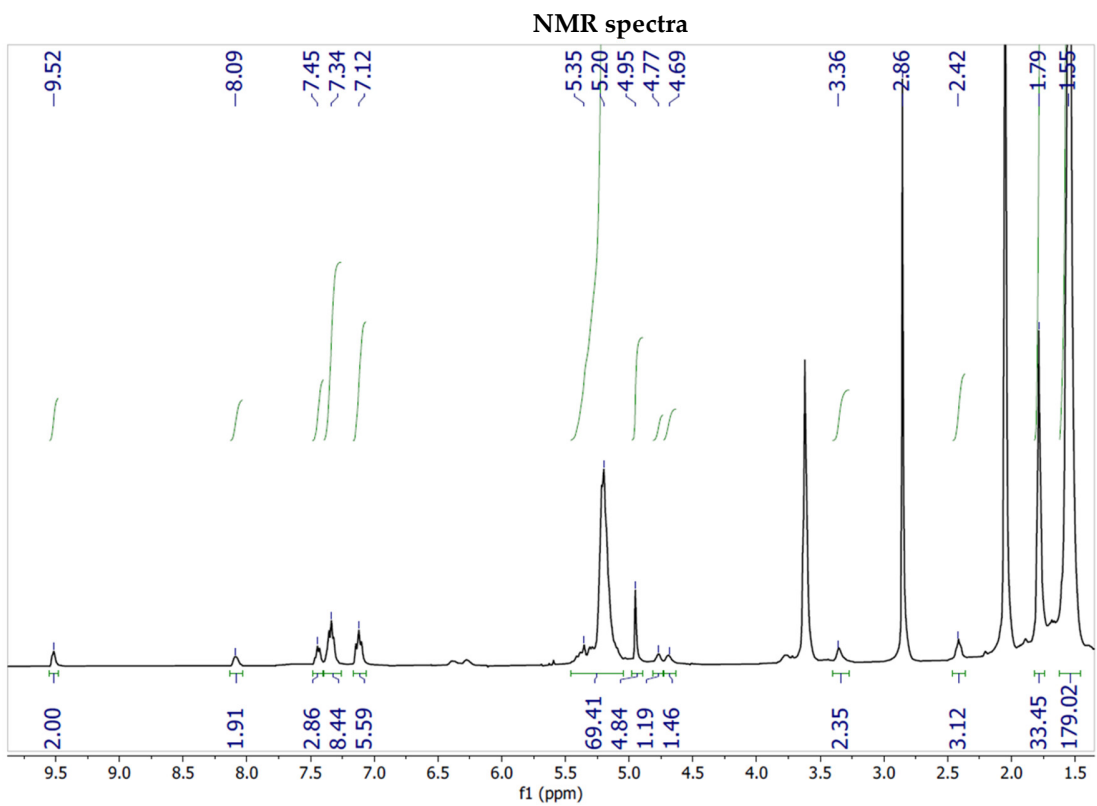


Figure S6. ^1H -NMR spectrum of complex **1** in acetone- d_6 at 298 K.

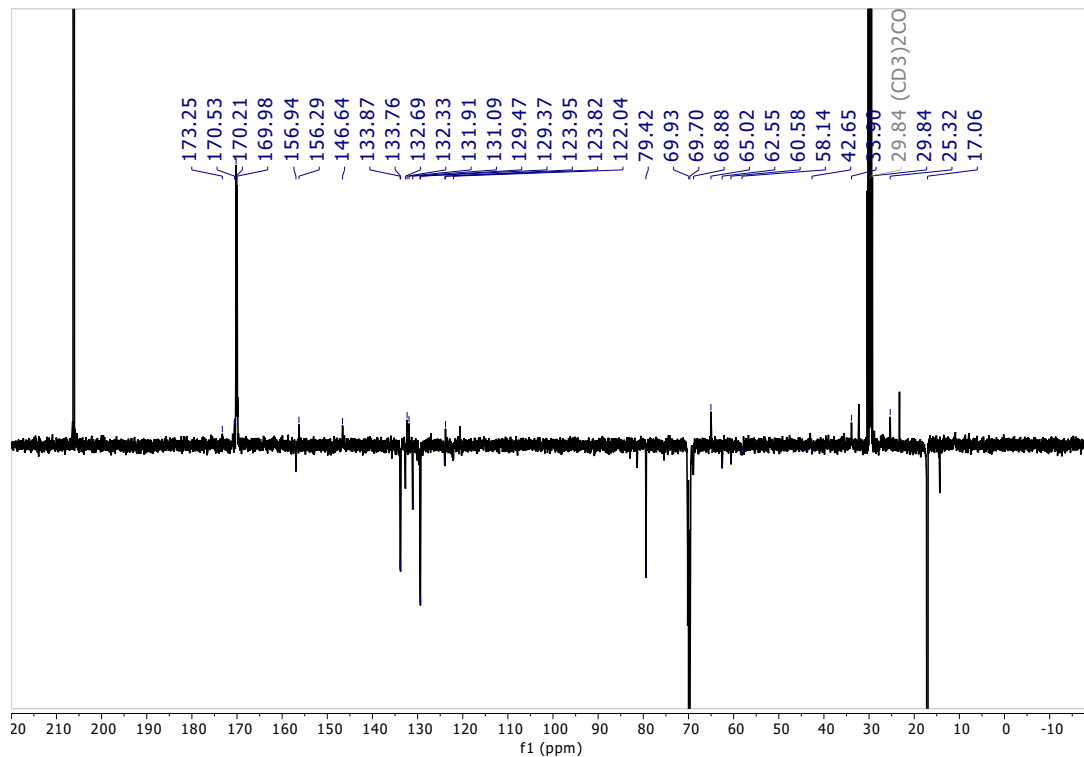


Figure S7. APT $^{13}\text{C}\{^1\text{H}\}$ -NMR spectrum of complex **1** in acetone- d_6 at 298 K.

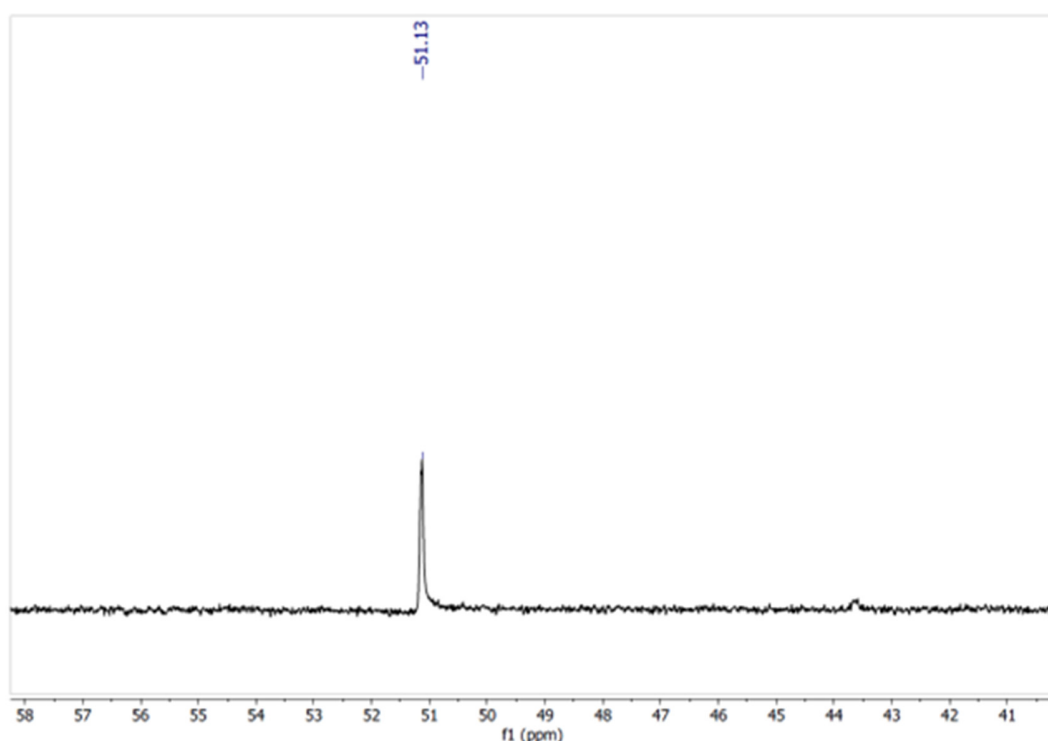


Figure S8. ³¹P{¹H}-NMR spectrum of complex 1 in acetone-*d*₆ at 298 K.

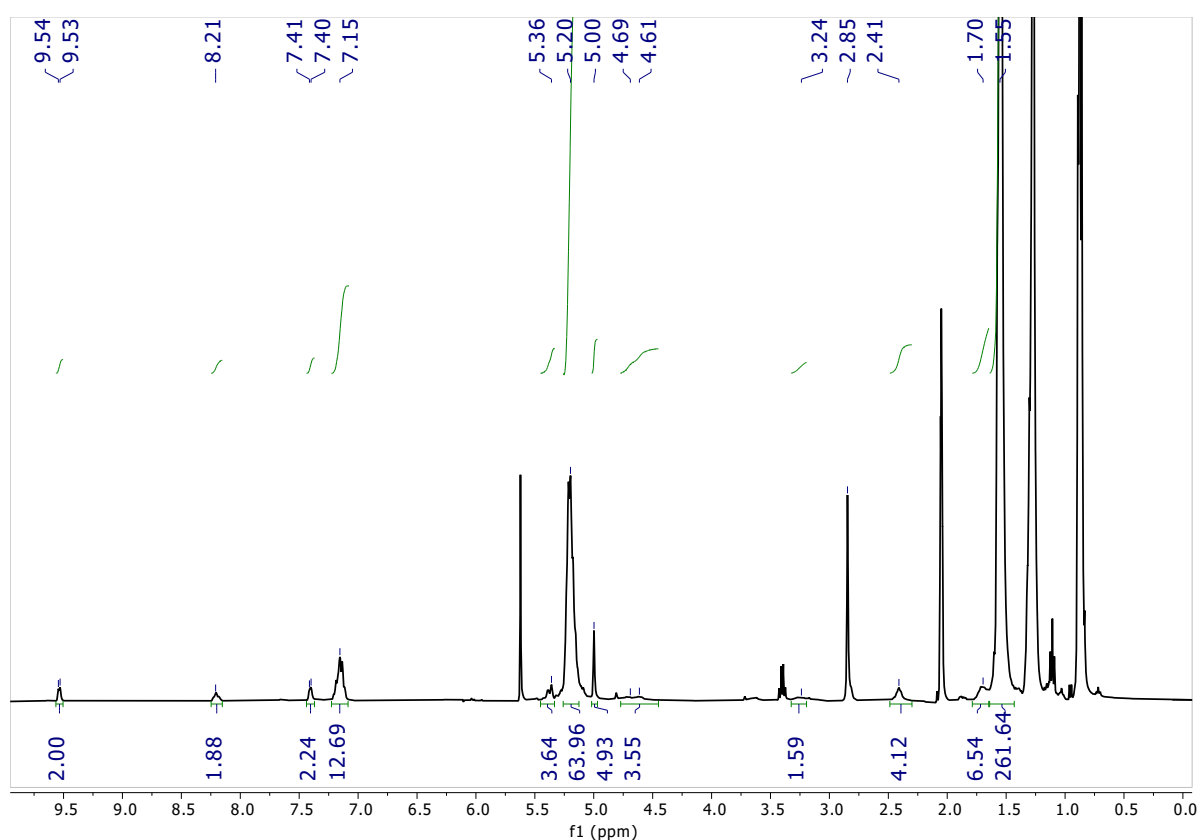


Figure S9. ¹H-NMR spectrum of complex 2 in acetone-*d*₆ at 298 K.

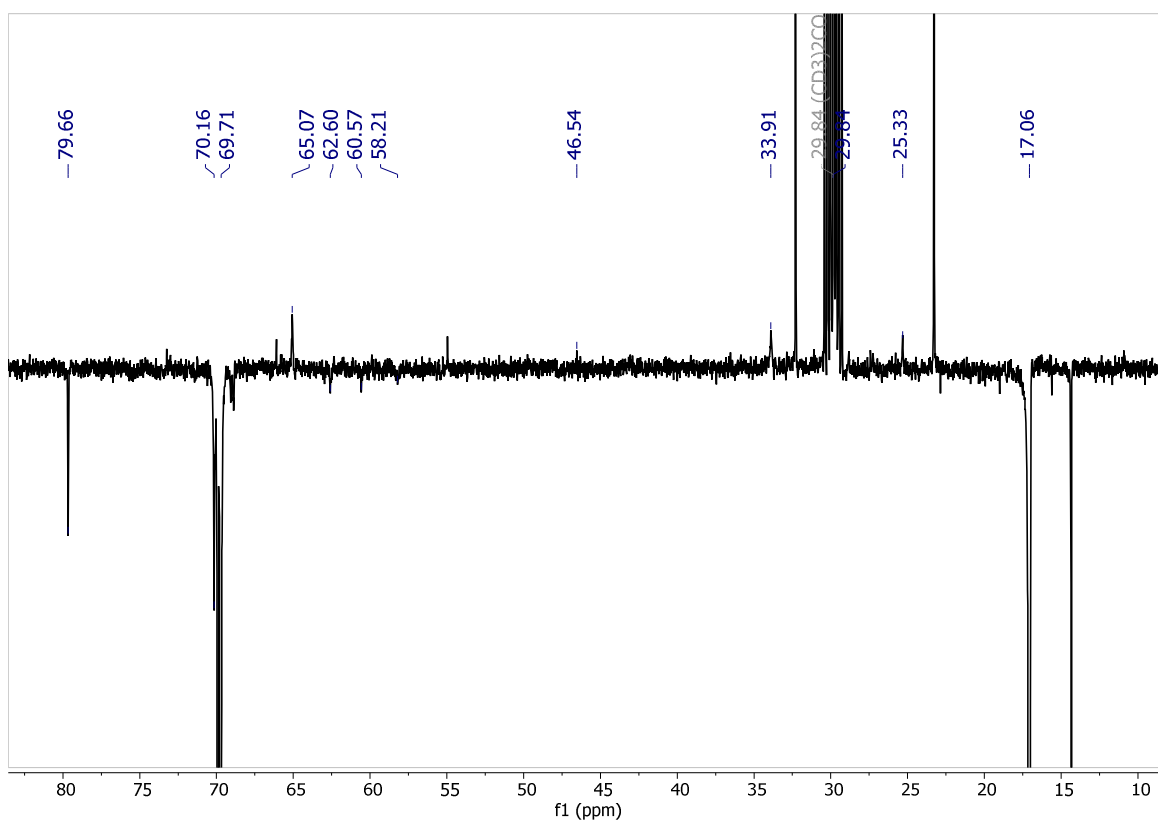


Figure S10. APT $^{13}\text{C}\{\text{H}\}$ -NMR spectrum of complex **2** in acetone- d_6 at 298 K.

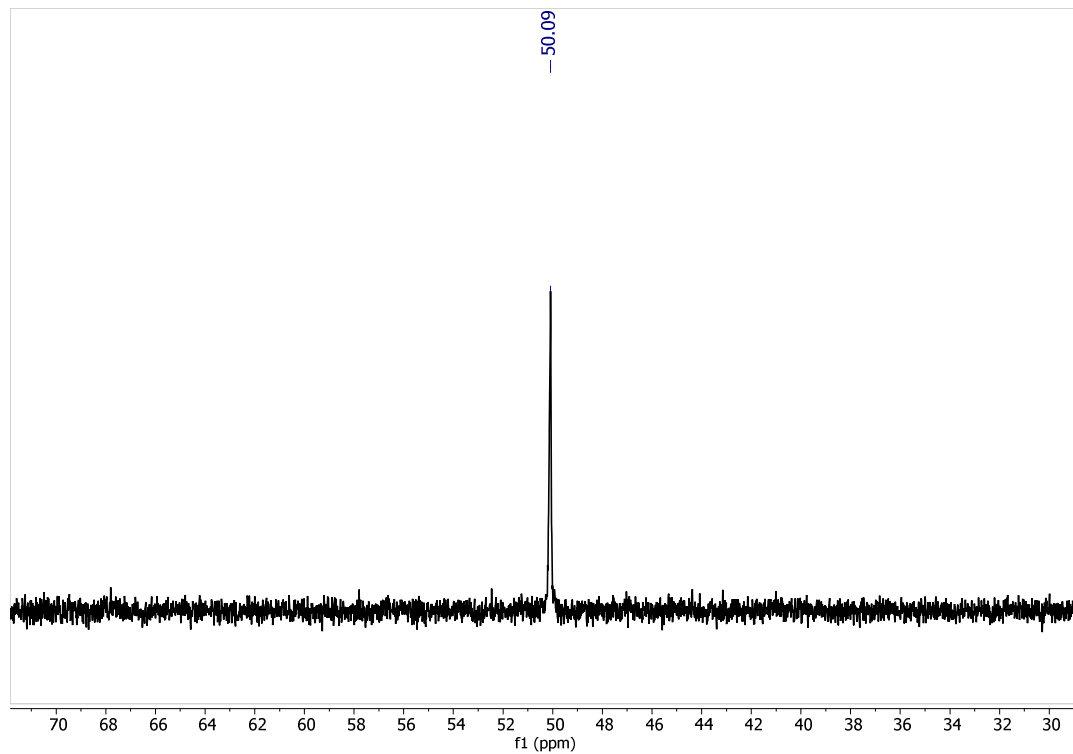


Figure S11. $^{31}\text{P}\{\text{H}\}$ -NMR spectrum of complex **2** in acetone- d_6 at 298 K.

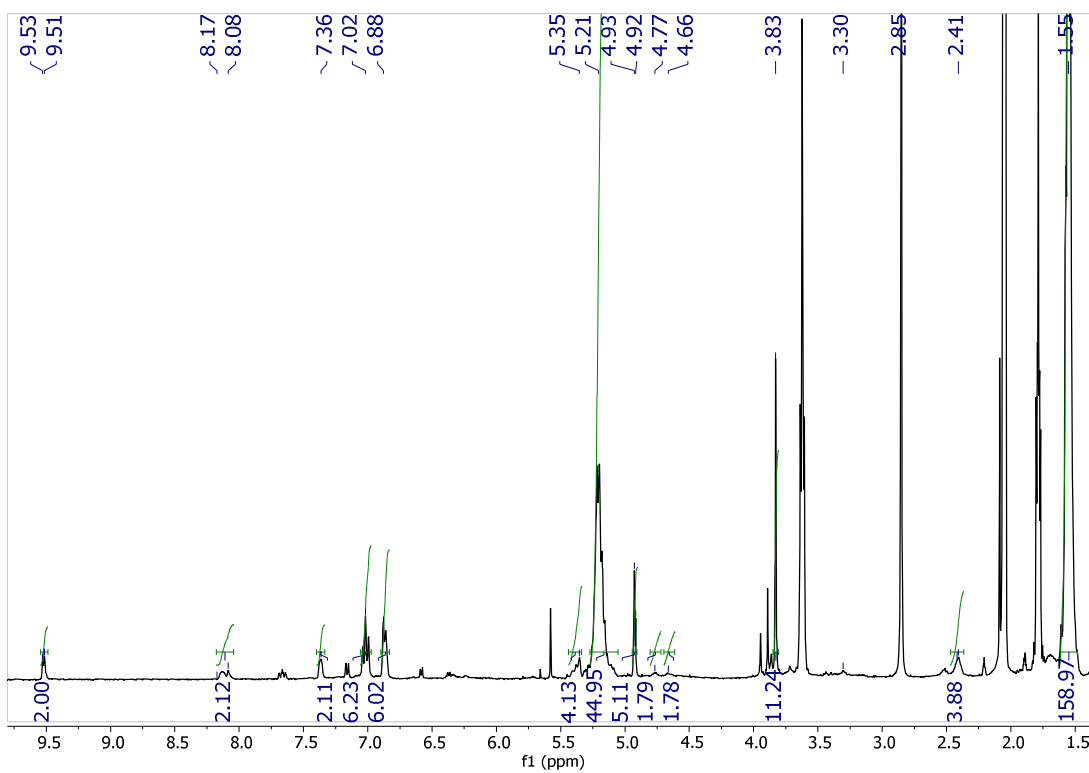


Figure S12. ^1H -NMR spectrum of complex **3** in acetone- d_6 at 298 K.

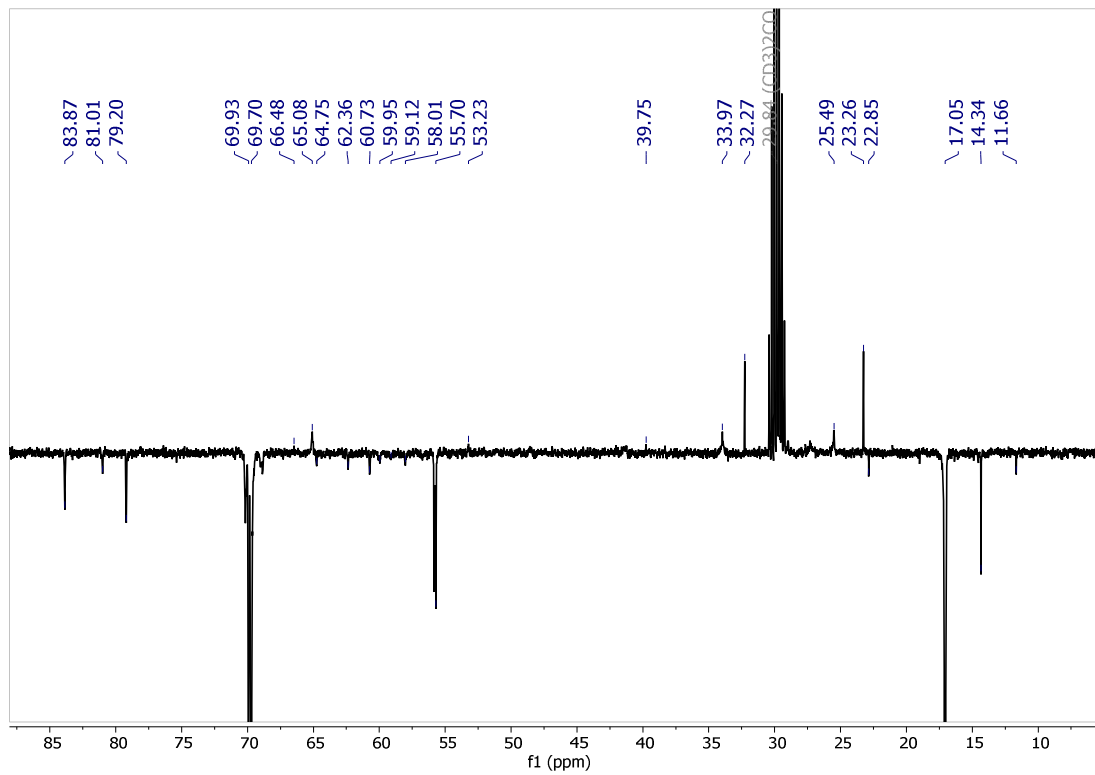


Figure S13. APT $^{13}\text{C}\{^1\text{H}\}$ -NMR spectrum of complex **3** in acetone- d_6 at 298 K.

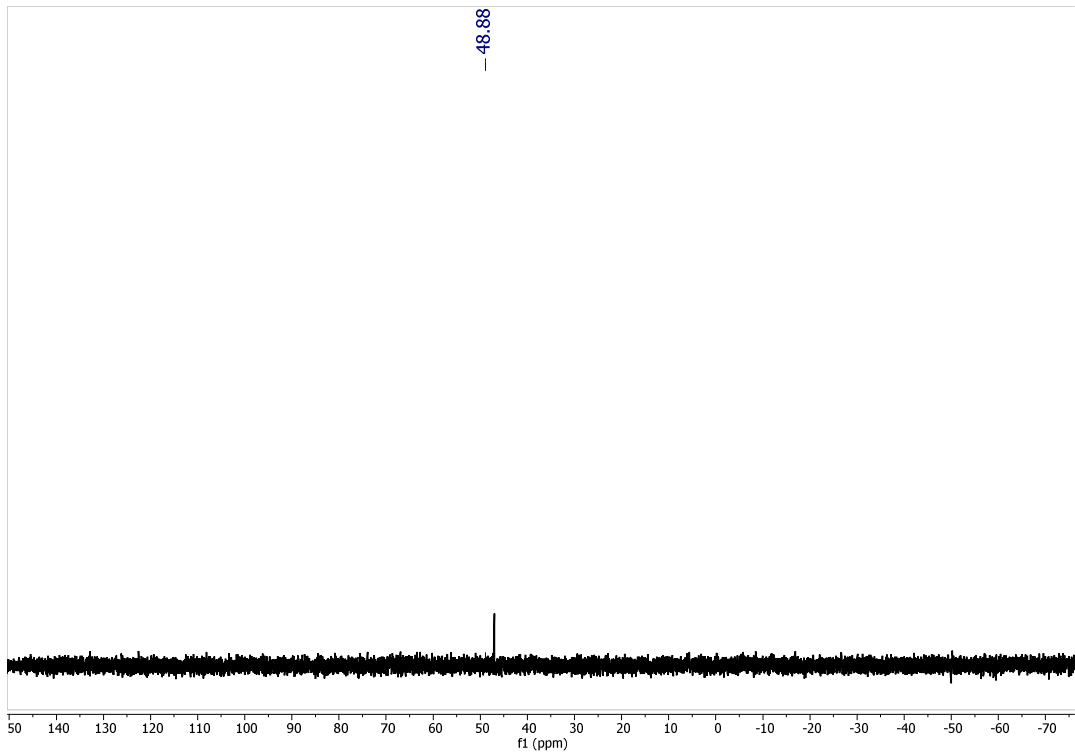


Figure S14. $^{31}\text{P}\{\text{H}\}$ -NMR spectrum of complex 3 in acetone- d_6 at 298 K.

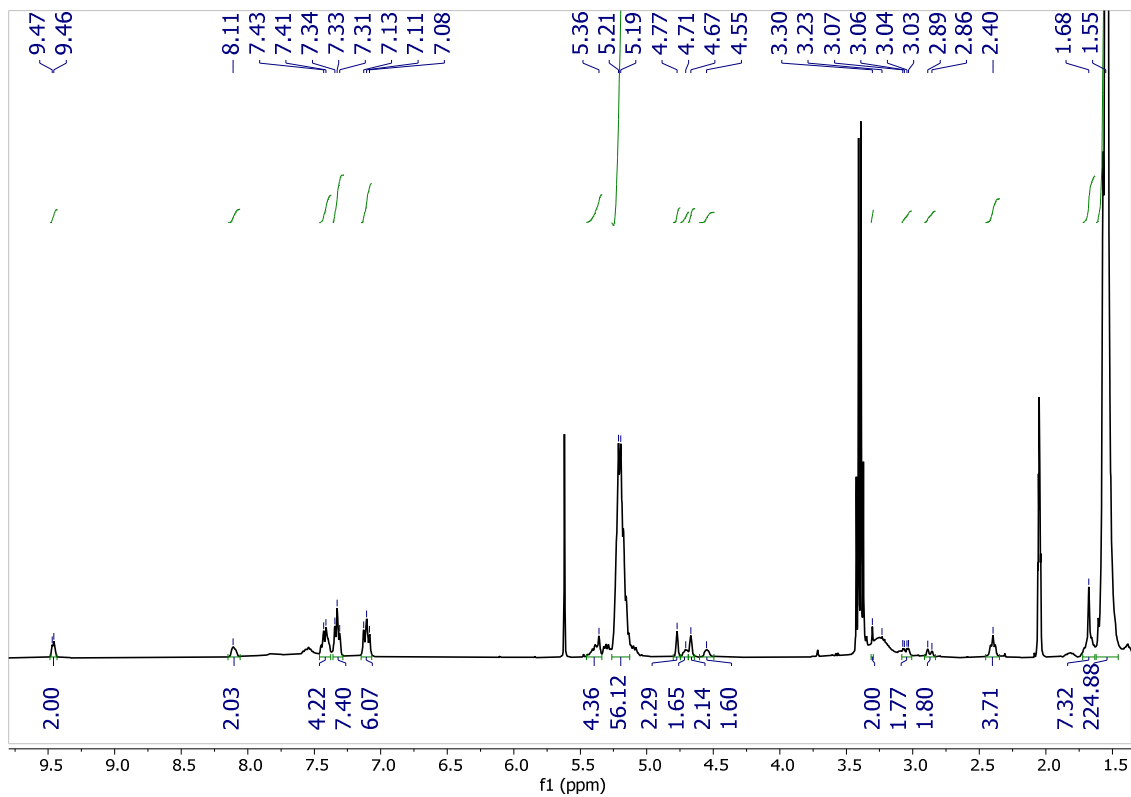


Figure S15. ^1H -NMR spectrum of complex 4 in acetone- d_6 at 298 K.

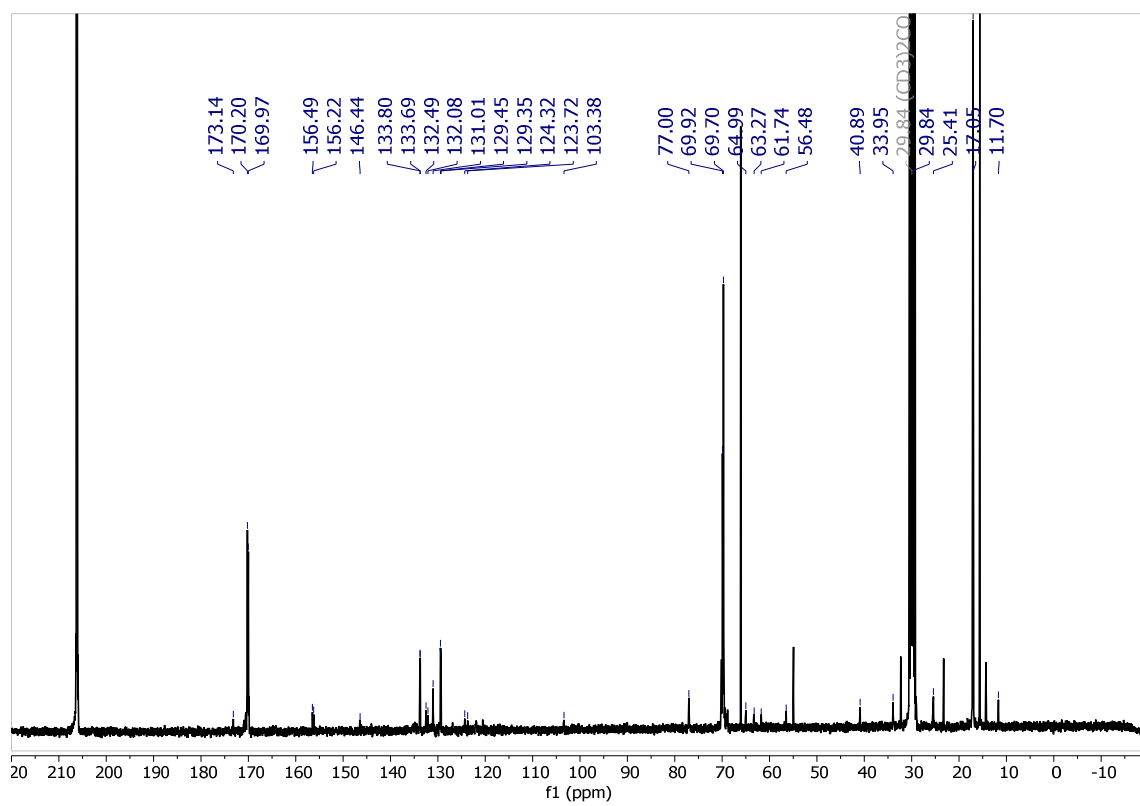


Figure S16. $^{13}\text{C}\{\text{H}\}$ -NMR spectrum of complex 4 in acetone- d_6 at 298 K.

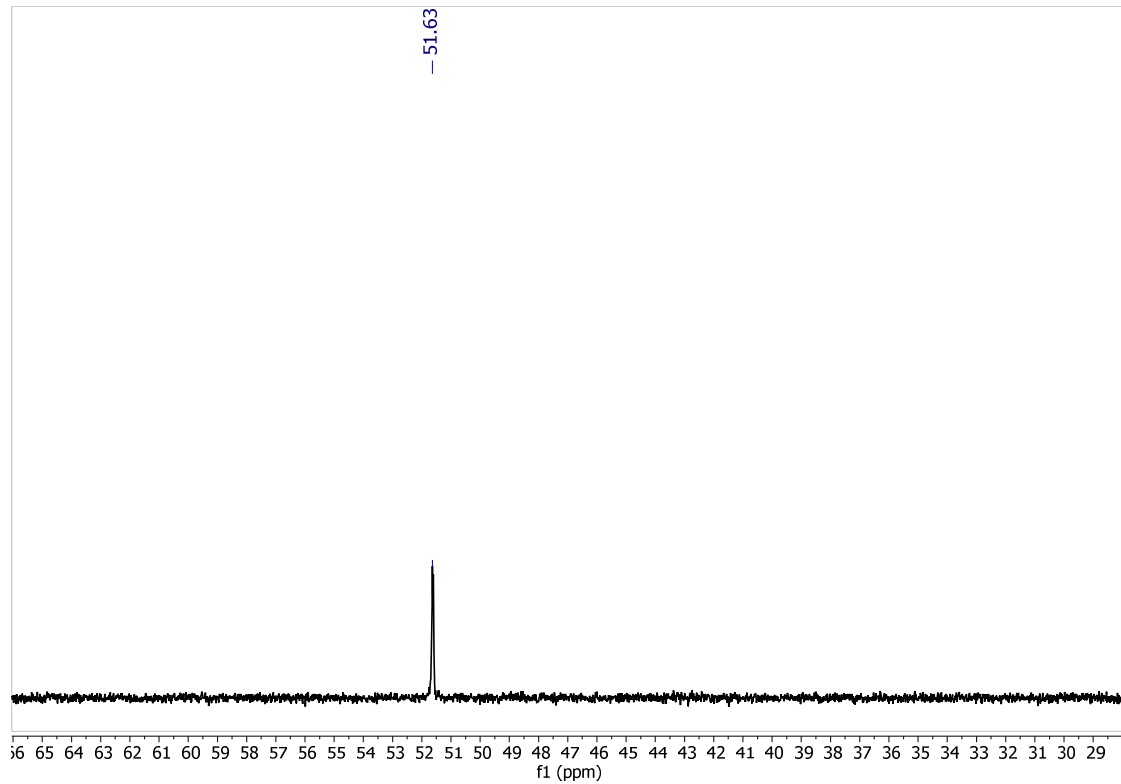


Figure S17. $^{31}\text{P}\{\text{H}\}$ -NMR spectrum of complex 4 in acetone- d_6 at 298 K.

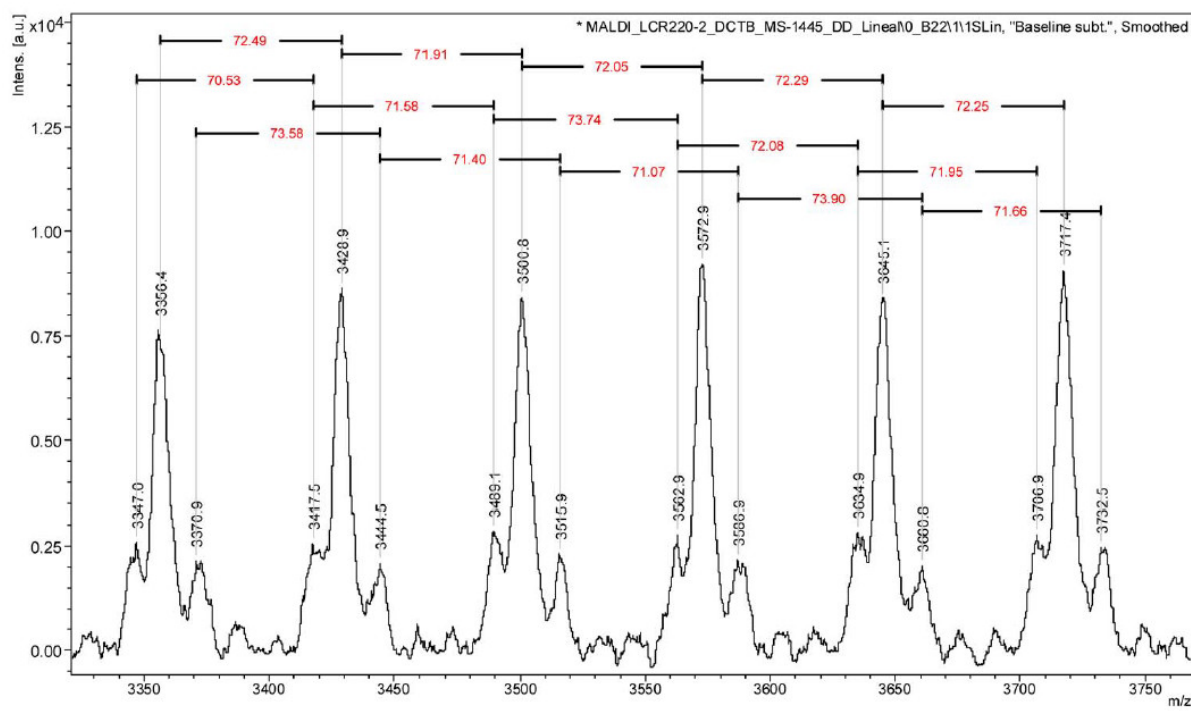
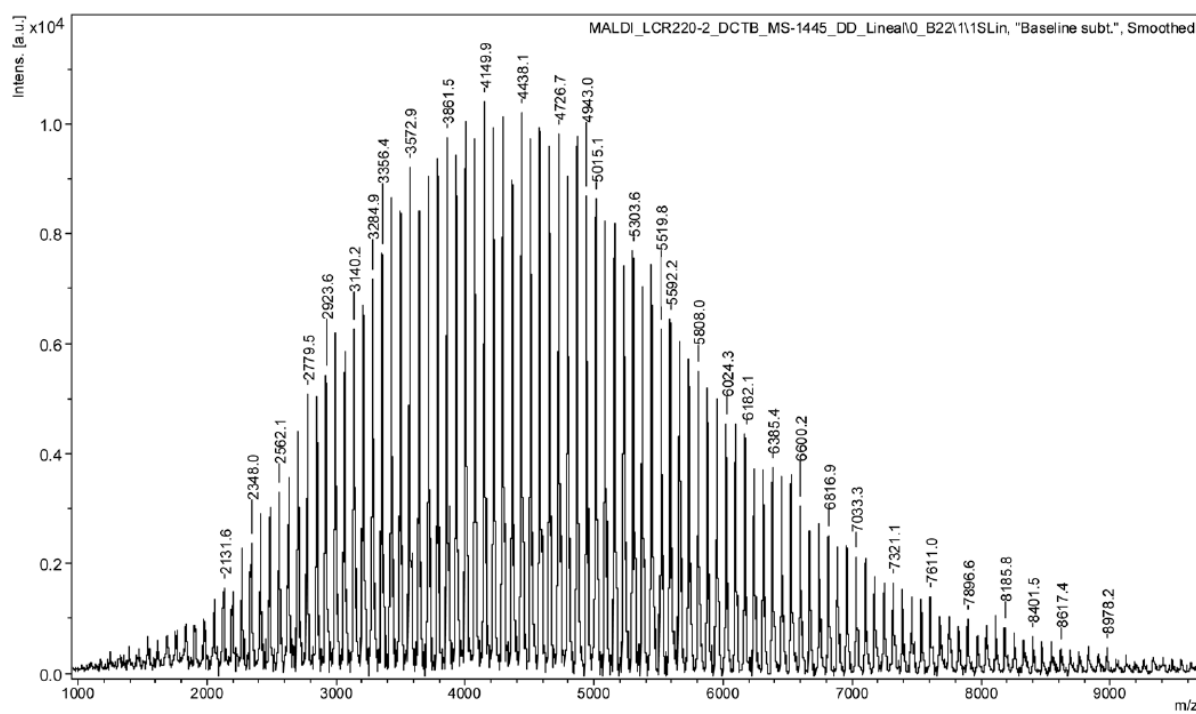


Figure S18. MALDI-TOF MS analysis of Compound 1.

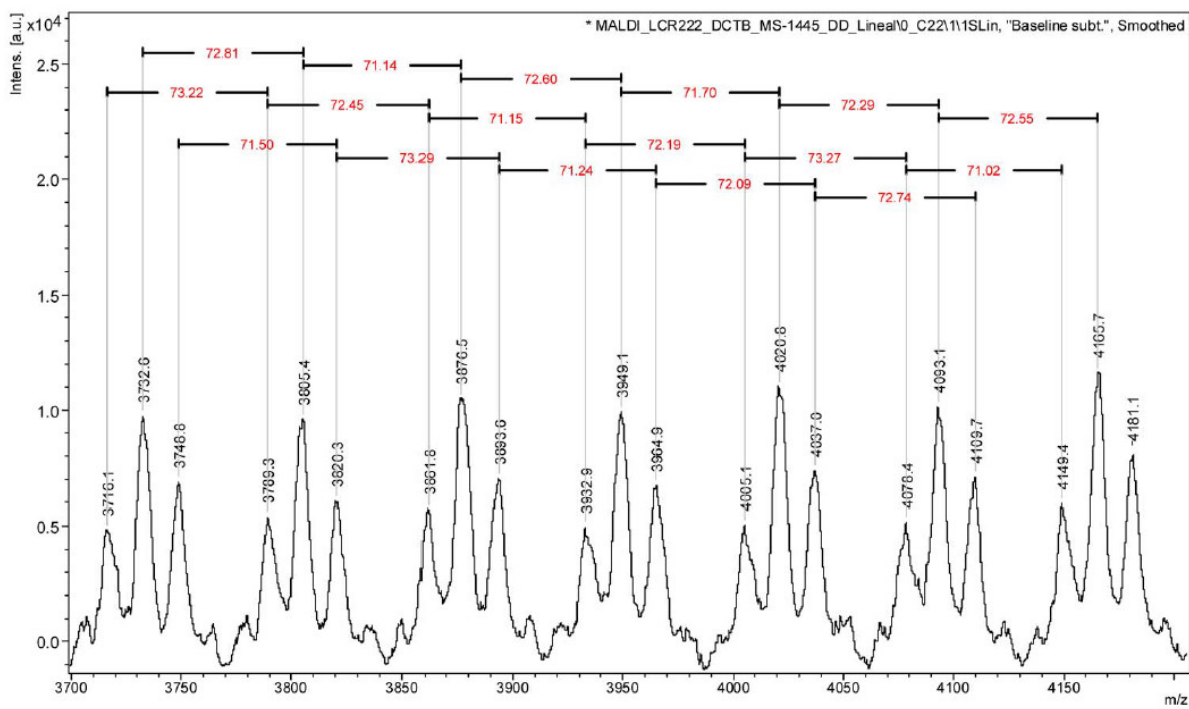
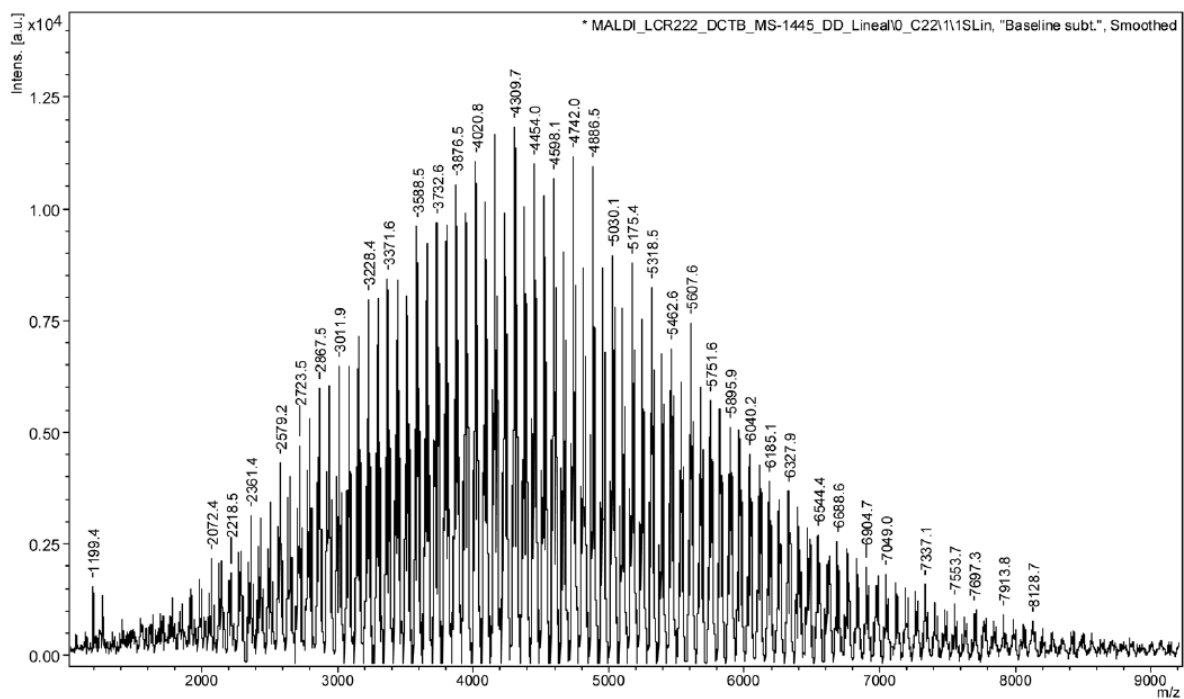


Figure S19. MALDI-TOF MS analysis of Compound 2.

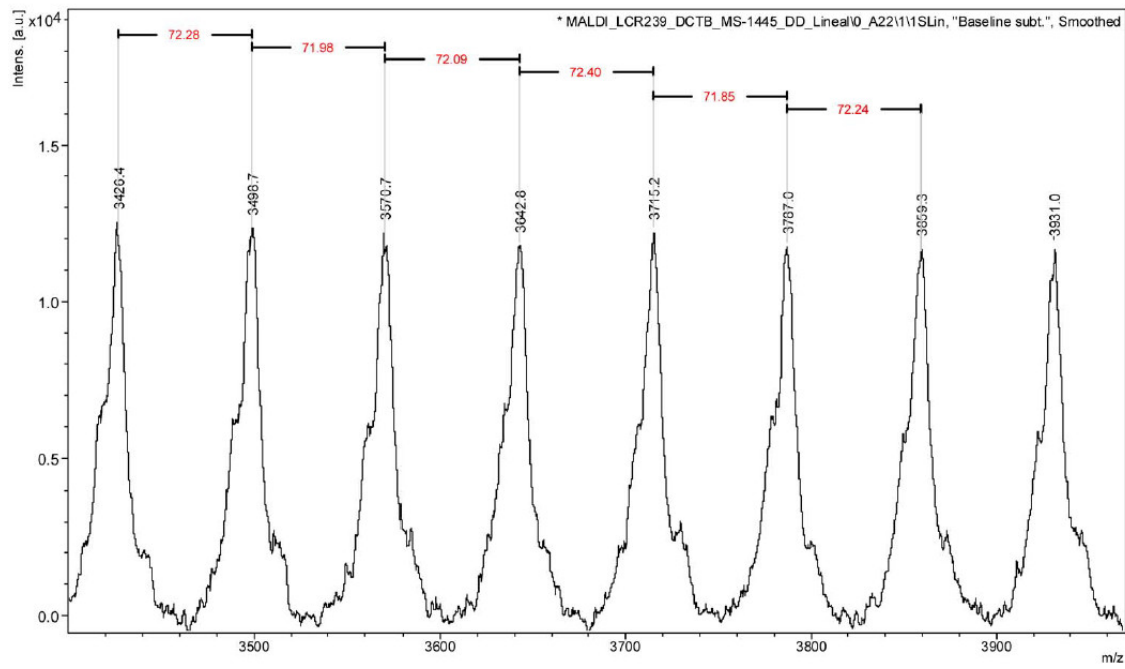
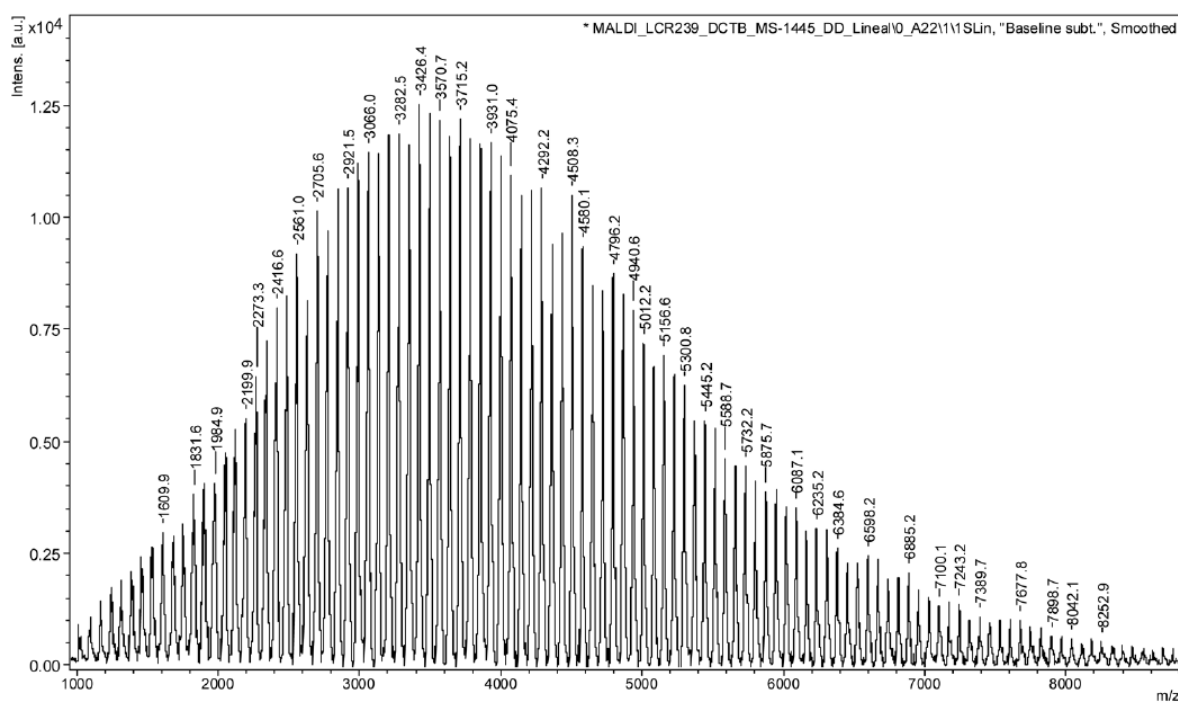


Figure S20. MALDI-TOF MS analysis of Compound 3.

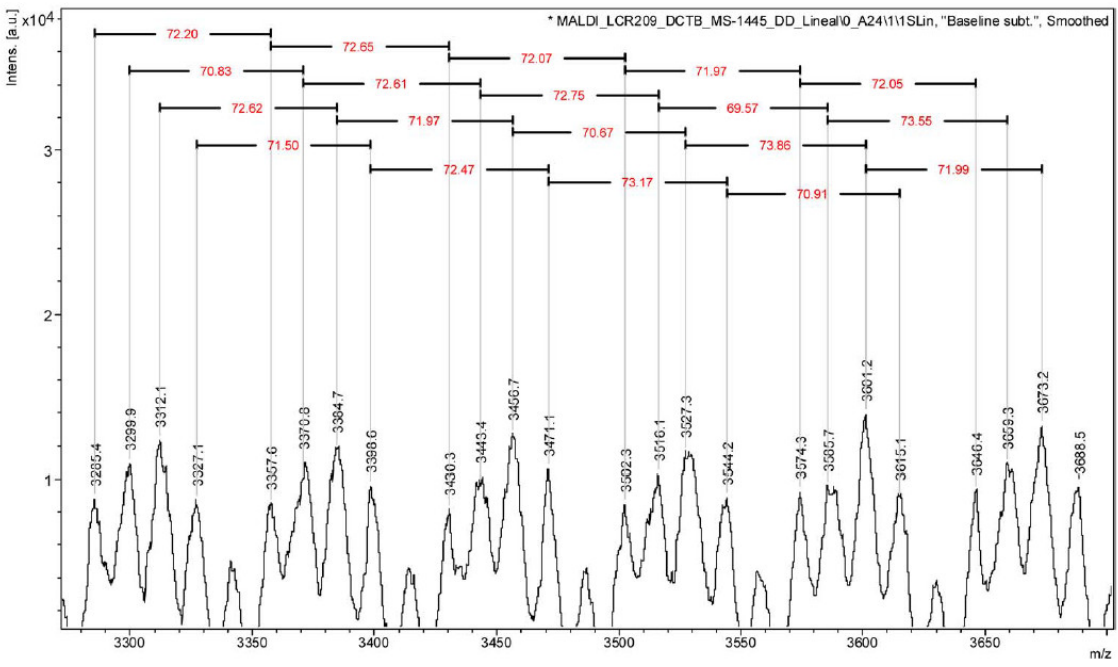
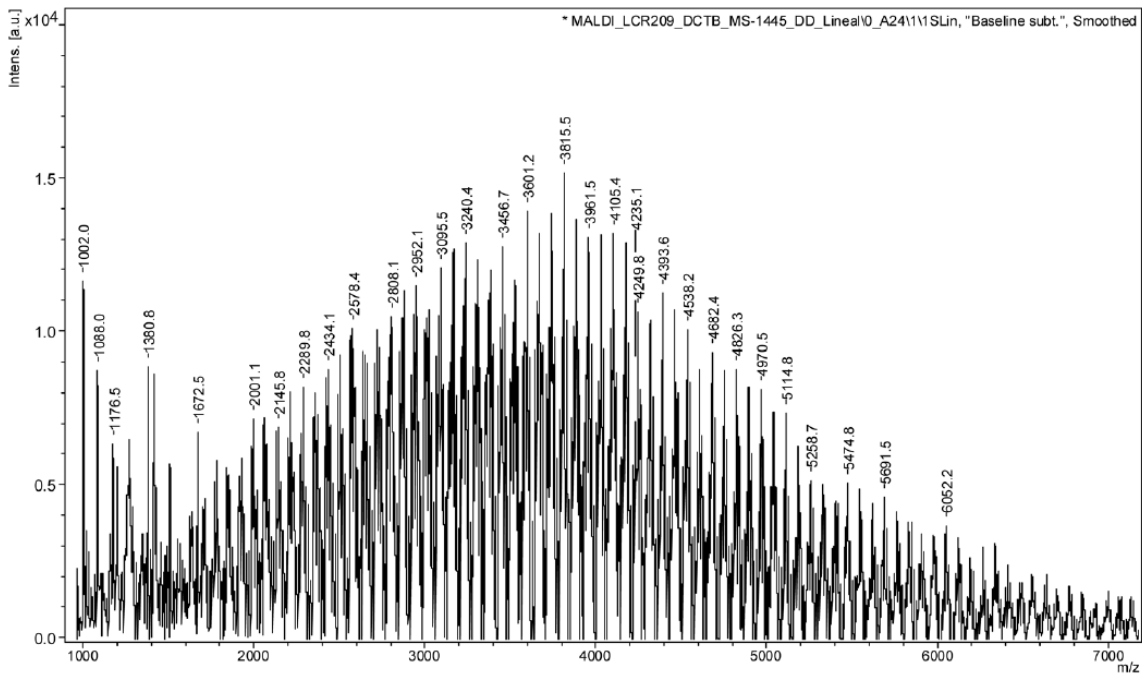


Figure S21. MALDI-TOF MS analysis of Compound 4.

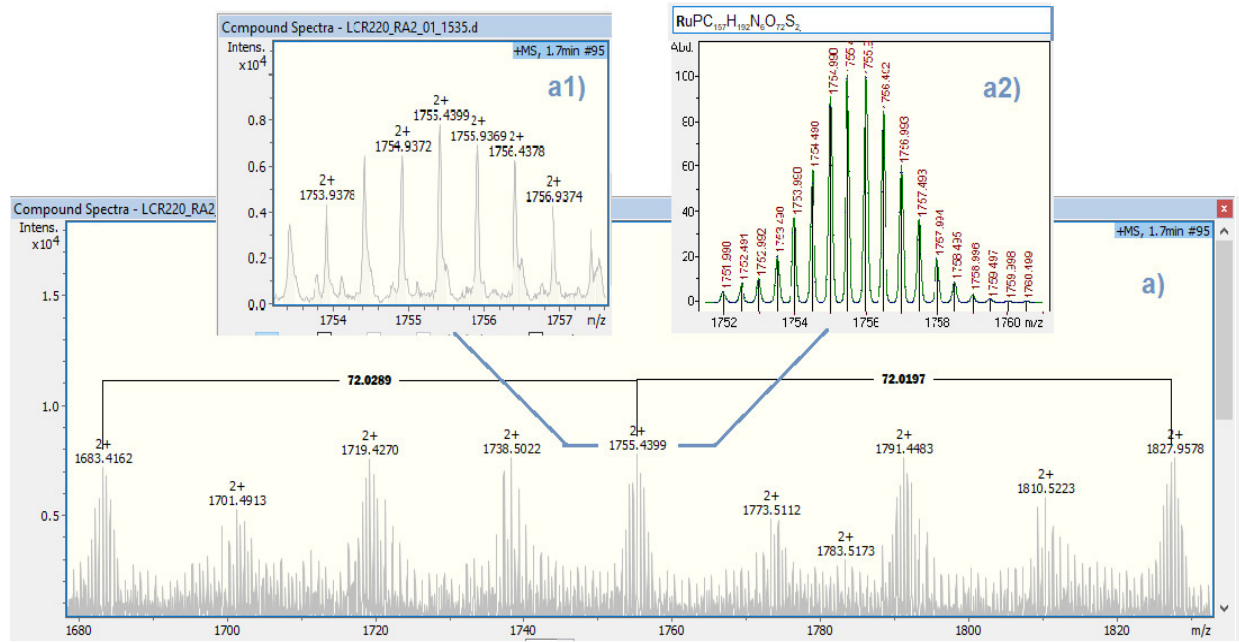


Figure S22. Partial HR mass spectrum obtained in the ESI positive mode of a methanolic solution of complex **1**. **a)** series of double charge ions attributed to $[\text{Ru}(\eta^5\text{-Cp})(\text{P}(\text{C}_6\text{H}_5)_3)(2,2'\text{-bipy-4,4'}\text{-(PLA)}_{n=16;17;18}\text{-biotin})]^{2+}$ structures spaced by 72.02 u; **a1)** the group of peaks at m/z 1755.44 assigned to $[\text{Ru}(\eta^5\text{-Cp})(\text{P}(\text{C}_6\text{H}_5)_3)(2,2'\text{-bipy-4,4'}\text{-(PLA)}_{n=16;17;18}\text{-biotin})]^{2+}$ exhibited a measured isotopic pattern as the calculated for the sum $[\text{RuPC}_{157}\text{H}_{192}\text{N}_6\text{O}_{72}\text{S}_2]^{2+}$ shown in **a2)**.

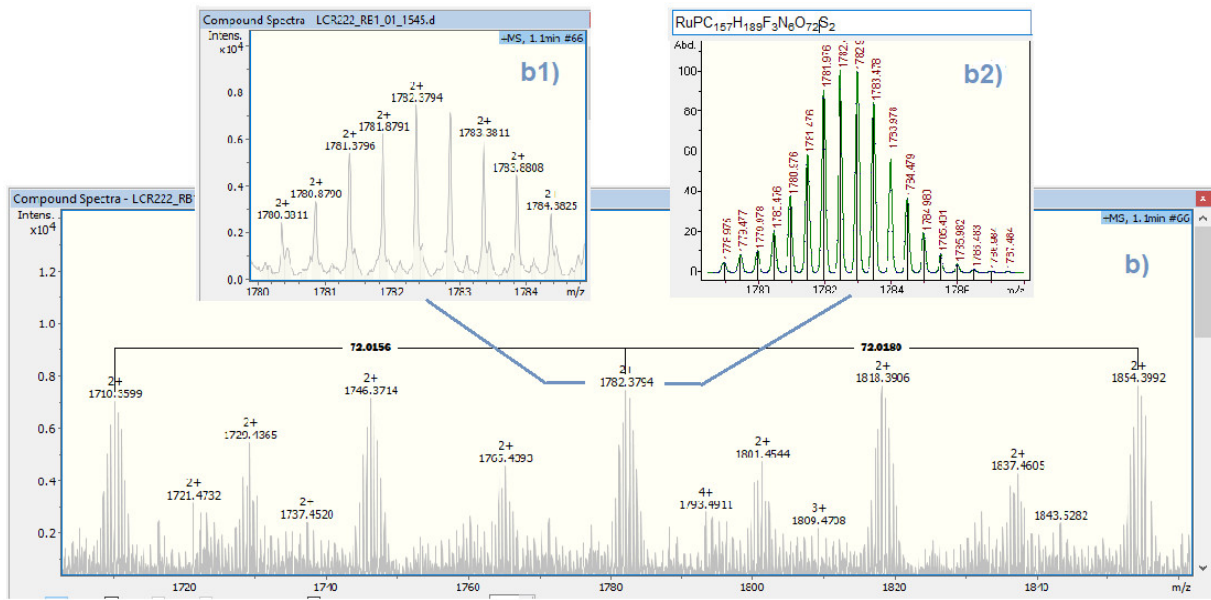


Figure S23. Partial HR mass spectrum obtained in the ESI positive mode of a methanolic solution of complex **2**. **b)** series of double charge ions attributed to $[\text{Ru}(\eta^5\text{-Cp})(\text{P}(\text{C}_6\text{H}_4\text{F})_3)(2,2'\text{-bipy-4,4'}\text{-(PLA)}_{n=16;17;18}\text{-biotin})]^{2+}$ structures spaced by 72.02 u; **b1)** the group of peaks at m/z 1782.47 exhibited a measured isotopic pattern as the calculated for the sum $[\text{RuPC}_{157}\text{H}_{189}\text{F}_3\text{N}_6\text{O}_{72}\text{S}_2]^{2+}$ shown in **b2**.

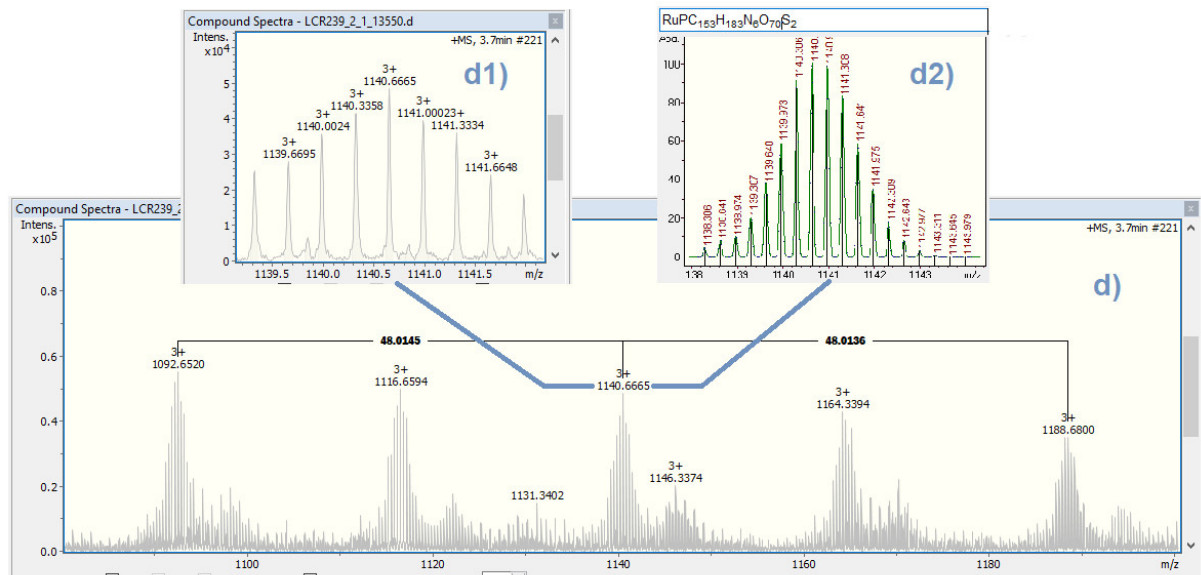


Figure S24. Partial HR mass spectrum obtained in the ESI positive mode of a methanolic solution of complex **3**. **d)** series of triple charge ions attributed to $[\text{Ru}(\eta^5\text{-Cp})(\text{P}(\text{C}_6\text{H}_4\text{OCH}_3)_3(2,2'\text{-bipy-4,4'}\text{-(PLA)}_{n=15;16;17}\text{-biotin})]^{3+}$ structures spaced by 48.01 u; **d1)** the group of peaks at m/z 1188.35 assigned to $[\text{Ru}(\eta^5\text{-Cp})(\text{P}(\text{C}_6\text{H}_4)_3(\text{CHO})_2)(2,2'\text{-bipy-4,4'}\text{-(PLA)}_{n=16}\text{-biotin})]^{3+}$ exhibited a measured isotopic pattern as the calculated for the sum $[\text{RuPC}_{153}\text{H}_{183}\text{N}_6\text{O}_{70}\text{S}_2]^{3+}$ shown in **d2)**.

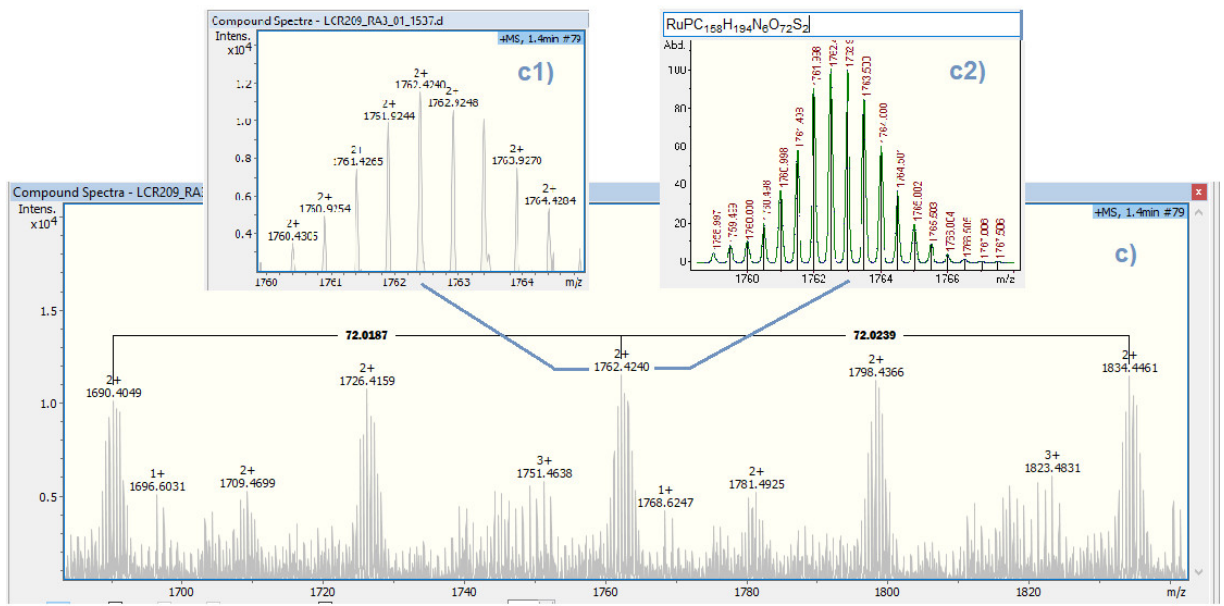


Figure S25. Partial HR mass spectrum obtained in the ESI positive mode of a methanolic solution of complex **4**. **c)** series of double charge ions attributed to $[\text{Ru}(\eta^5\text{-CpCH}_3)(\text{P}(\text{C}_6\text{H}_5)_3)(2,2'\text{-bipy-4,4}'\text{-(PLA)}_{n=16;17;18}\text{-biotin})]^{2+}$ structures spaced by 72.02 u; **c1)** the group of peaks at m/z 1762.42 assigned to $[\text{Ru}(\eta^5\text{-CpCH}_3)(\text{P}(\text{C}_6\text{H}_5)_3)(2,2'\text{-bipy-4,4}'\text{-(PLA)}_{n=16;17;18}\text{-biotin})]^{2+}$ exhibited a measured isotopic pattern as the calculated for the sum $[\text{RuPC}_{158}\text{H}_{194}\text{N}_6\text{O}_{72}\text{S}_2]^{2+}$ shown in **c2)**.

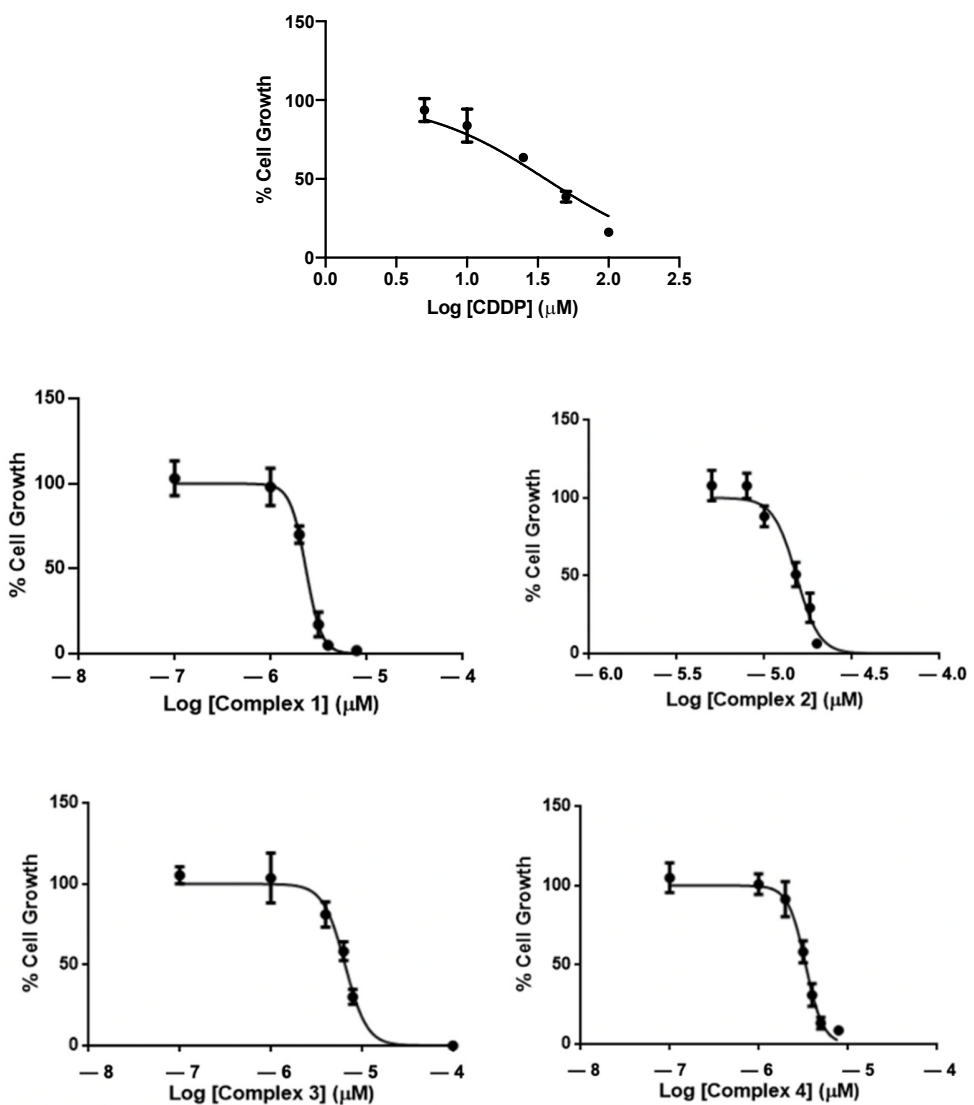


Figure S26. Dose-response curve of cell viability in MDA-MB-231 cell line for determination of IC₅₀ by MTT (complexes 1-4) or Sulforhodamine B (Cisplatin) after 48 h incubation.

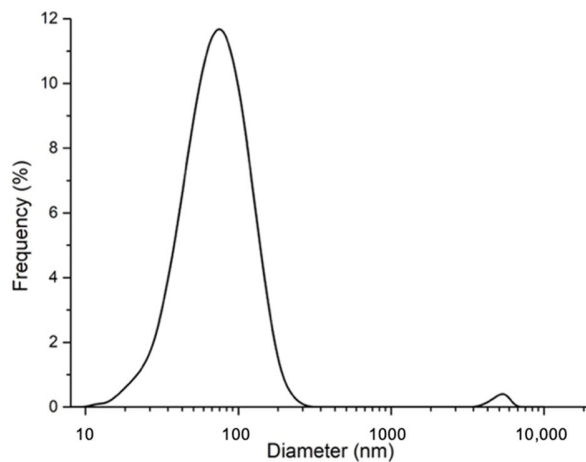


Figure S27. Hydrodynamic diameter distribution (obtained by DLS) of complex 1.

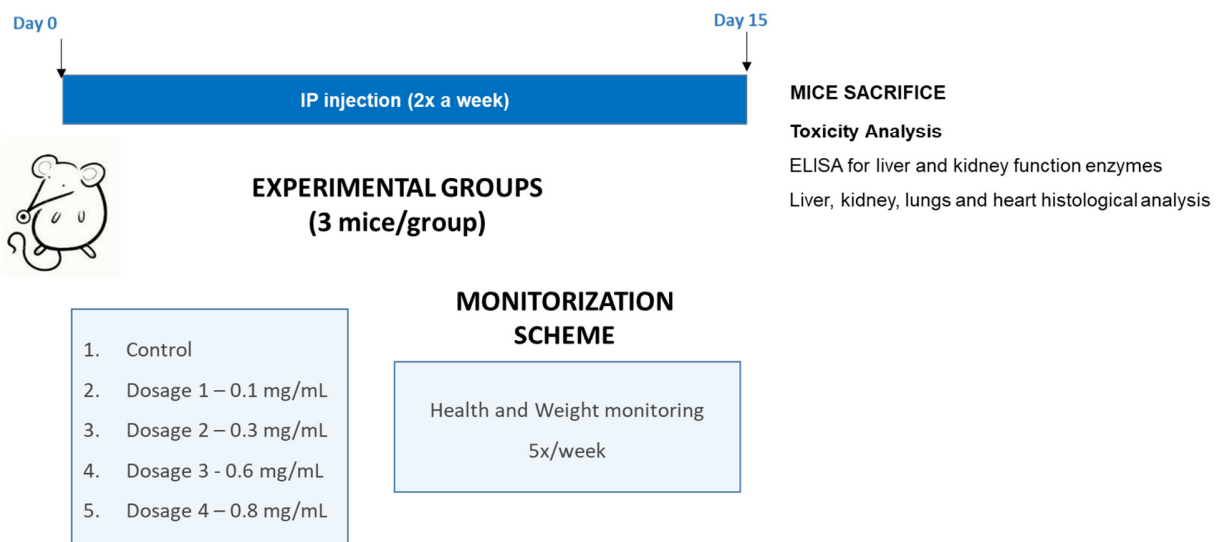


Figure S28. Experimental design of toxicology assay performed.

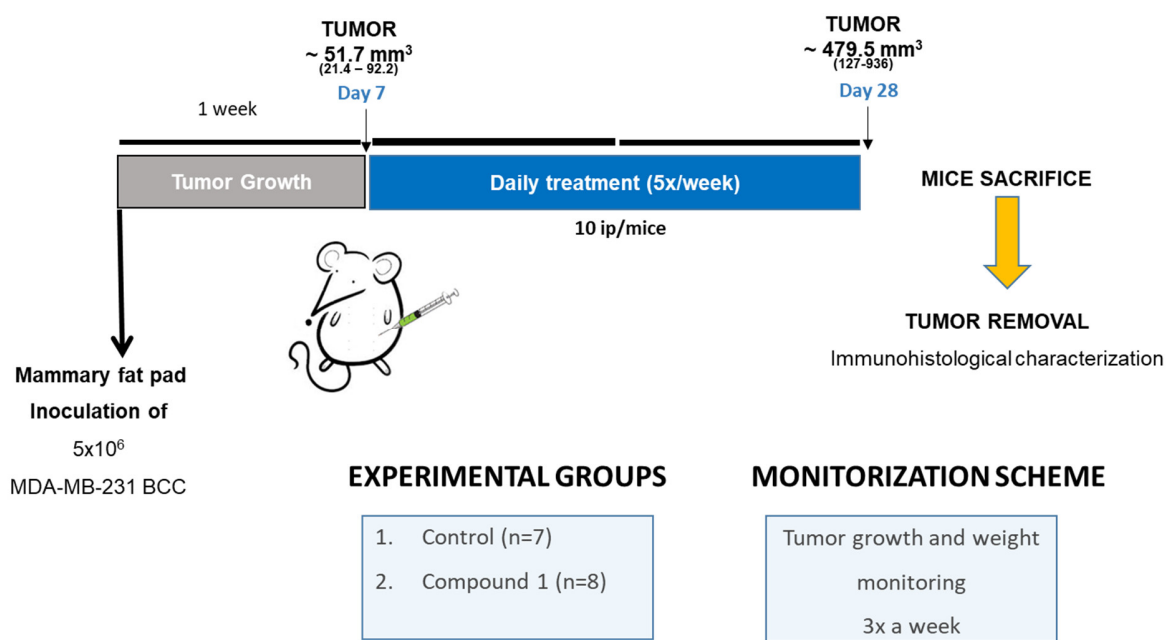


Figure S29. Experimental design of tumor growth assay.